Spectrochimica Acta Part A: Molecular and Biomolecular Spectroscopy 230 (2020) 118071

Contents lists available at ScienceDirect

Spectrochimica Acta Part A: Molecular and Biomolecular Spectroscopy

journal homepage: www.elsevier.com/locate/saa

Laser heterodyne spectroradiometer assisted by self-calibrated wavelength modulation spectroscopy for atmospheric CO_2 column absorption measurements

Hao Deng [a,b], Mingxing Li [a,b], Yabai He [a], Zhenyu Xu [a], Lu Yao [a], Bing Chen [a], Chenguang Yang [a,*], Ruifeng Kan [a,c,**]

[a] Key Laboratory of Environmental Optics and Technology, Anhui Institute of Optics and Fine Mechanics, Chinese Academy of Sciences, Hefei, Anhui 230031, China
[b] University of Science and Technology of China, Hefei, Anhui 230022, China
[c] Changchun Institute of Optics, Fine Mechanics and Physics, Chinese Academy of Sciences, Changchun 130033, China

ARTICLE INFO

Article history:
Received 6 September 2019
Received in revised form 29 November 2019
Accepted 11 January 2020
Available online 13 January 2020

Keywords:
Laser heterodyne spectroradiometer
Wavelength modulation spectroscopy
Carbon dioxide
Column concentration
Optical sensing

ABSTRACT

We have developed a laser heterodyne spectroradiometer in combination with self-calibrated wavelength modulation spectroscopy based on a software-based lock-in amplifier to observe the atmospheric carbon dioxide (CO_2) column absorption near wavelength 1.57 μm in solar occultation mode. This combination facilitates miniaturization of laser heterodyne radiometer. Combined with our developed retrieval algorithm, the atmospheric carbon dioxide column concentration is measured to be 413.7 ± 1.9 ppm, in agreement with GOSAT satellite observation results. This system offers high spectral signal-to-noise ratio of ~333 for the zeroth harmonic (0f) normalized second harmonic (R2f) signal of CO_2 transition (R22e), with a measurement averaging time of 8 s, which can be further improved by increasing averaging time in accordance to the Allan deviation analysis for the noise fluctuation. This demonstrates the feasibility of the system for atmospheric investigation and the potential of ground-based, airborne and spaceborne observations for the variation of the global greenhouse gases.

1. Introduction

Laser heterodyne radiometer (LHR) is a powerful tool for earth atmospheric remote sensing [1–10] due to its advantages of ultrahigh resolution and high sensitivity. These reported LHR detected the heterodyne signals by firstly modulating the sunlight or signal light with a mechanical chopper or optical switch, and then using a lock-in amplifier for demodulation to achieve high signal-to-noise ratio (SNR). This measurement approach is analog to a basic absorption spectroscopy measurement. Therefore, various advanced laser spectroscopy techniques might be adopted to improve the measurement sensitivity of LHR further.

One recent development was to apply wavelength modulation spectroscopy (WMS) technique in LHR, as reported by Pedro Martin-Mateos et al. [11,12], which also enabled a simplification of the optical layout of the system to some extent. The research results indicated that the performance of the wavelength modulation LHR was better than that of the conventional LHR. However, the WMS-LHR has not been tested in practical applications yet, such as in atmospheric greenhouse gases measurements. There are two main kinds of WMS techniques: traditional WMS [13–17] and the so-called self-calibrated (or calibration-free) WMS [18–21]. While traditional WMS requires calibration measurements for its signal dependence on absorbance, this later technique was based on accurate characterizations of laser intensity and wavelength scan. The concentration of the target species can then be retrieved by fitting simulated harmonic signals to the experimental signal under known environmental parameters, such as temperature and pressure of the target species.

In this paper, we report on a development and demonstration of a self-calibrated wavelength modulation LHR to measure the column absorption of carbon dioxide (CO_2) near wavelength 1.57 μm in solar occultation mode. To our best knowledge, application of self-calibrated WMS for LHR in atmosphere measurements has not been reported yet. Furthermore, we replaced hardware-based lock-in amplifier used

* Corresponding author.
** Correspondence to: R. Kan, Key Laboratory of Environmental Optics and Technology, Anhui Institute of Optics and Fine Mechanics, Chinese Academy of Sciences, Hefei, Anhui 230031, China.
E-mail addresses: cgyang@aiofm.ac.cn (C. Yang), rfkan@ciomp.ac.cn (R. Kan).

https://doi.org/10.1016/j.saa.2020.118071
1386-1425/

in conventional LHR by a software-based lock-in amplifier for demodulating the harmonic signal, which vastly minimized the size of the system.

2. Experimental details

The schematic diagram of our experimental arrangement is displayed in Fig. 1. The sunlight was collected into a single-mode optical fiber by using an off-axis parabolic collimator (RC08FC-P01, Thorlabs). A near-infrared distributed feedback (DFB) diode laser (NLK1L5GAAA, NEL) operating near 1.571 μm wavelength was served as the local oscillator for heterodyne detection. This laser light was mixed with the sunlight to make a selective interference interaction for narrowband detection of the sunlight component around the laser wavelength/frequency. Sensitive high-resolution sunlight atmospheric absorption spectra will be acquired by scanning the laser wavelength/frequency. The diode laser operation current was controlled via a 16 bit & 2 MSamp/s data acquisition card (USB-6363, National Instruments), which was programmed to generate a superimposed low frequency (125 Hz) sawtooth wavelength scan signal with a high frequency (41.22 kHz) sinusoidal modulation signal. The laser output radiation was divided into two beams by a single-mode fiber splitter. The main laser beam was superimposed with the collected sunlight through a single-mode fiber coupler (F-CPL-F12131, Newport). Then their mixing and interaction were detected by a 5-GHz fast InGaAs photodetector (DET08CFC/M, Thorlabs) to produce radio frequency (RF) heterodyne beat signals. A bias-tee was used as an ac-coupler to block out the direct current term contained in the beat signal. The ac-coupled signal passed through a four-stage RF amplifier. The effective bandwidth of the combined photodiode-amplifiers for the heterodyne beat signal was 1 GHz. This was determined using a tunable heterodyne beat signal, which was generated by temporarily replacing the broadband sunlight with a tunable narrowband external-cavity diode laser (ECDL). The power level of the amplified RF heterodyne beat signal was measured by a RF power detector based on a Schottky diode. The Schottky diode converted RF power to a voltage output signal, which was recorded at 2 MSamp/s via the data acquisition card (DAQ 1).

During WMS-LHR, the second harmonic signal of the DFB laser modulation contained in the heterodyne RF power (recorded by DAQ 1) was demodulated by a software-based lock-in amplifier programmed in Python on a computer board. The second harmonic amplitude (R2f) was subject to absorption loss of sunlight by atmospheric gas species. Simultaneously, the laser frequency change/scan was determined by measuring the interference fringe signals produced by the second laser beam passing through a quartz Fabry-Parot etalon and recorded via another 12 bit & 60 MSamp/s data acquisition card (DAQ 2).

3. Data retrieval details and results of analysis

3.1. Principle of self-calibrated WMS-LHR

The principle of a laser heterodyne detection has been briefly described in our previous study [10]. Herein, the local oscillator and the signal light are considered as perfectly aligned plane waves

$$E_{LO}(t) = A_{LO}\cos(\omega_{LO}t + \phi) \tag{1}$$

and

$$E_s(t) = A_s\cos(\omega_s t) \tag{2}$$

where $E_{LO}(t)$ and $E_s(t)$ refer to the fields of the local oscillator and the signal light at time t, ω_{LO} and ω_s refer to angular frequencies of the fields, A_{LO} and A_s refer to amplitudes of the fields, ϕ refers to phase term of the field of the local oscillator. When both fields of the $E_{LO}(t)$ and $E_s(t)$ were mixed on a square-law photodiode detector, the generated response current of the detector can be represented by:

$$i(t) = \kappa(E_{LO}(t) + E_S(t))^2 \tag{3}$$

where κ is detector's sensitivity. The above equation can be expressed as:

$$\begin{aligned} i'(t) = \kappa\Big\{ & A_sA_{LO}\cos[(\omega_{LO}+\omega_s)t+\phi] + \frac{1}{2}A_s^2(1+\cos 2\omega_s t) \\ & + \frac{1}{2}A_{LO}^2[1+\cos 2(\omega_{LO}t+\phi)] + A_sA_{LO}[\cos(\omega_{LO}-\omega_s)t+\phi]\Big\} \end{aligned} \tag{4}$$

The high-frequency terms of $A_sA_{LO}[\cos(\omega_{LO}+\omega_s)t+\phi]$, $\frac{1}{2}A_s^2\cos 2\omega_s t$ and $\frac{1}{2}A_{LO}^2\cos(2\omega_{LO}t+\phi)$, will not be responded by the detector due to its bandwidth limitation, so they can be ignored. The Eq. (4) can be simplified as:

$$i''(t) = \kappa\left\{\frac{1}{2}A_s^2 + \frac{1}{2}A_{LO}^2 + A_sA_{LO}[\cos(\omega_{LO}-\omega_s)t+\phi]\right\} \tag{5}$$

where $\frac{1}{2}A_s^2$ and $\frac{1}{2}A_{LO}^2$ are direct current (DC) terms, and $A_sA_{LO}[\cos(\omega_{LO}-\omega_s)t+\phi]$ is an intermediate frequency (IF) term. In the

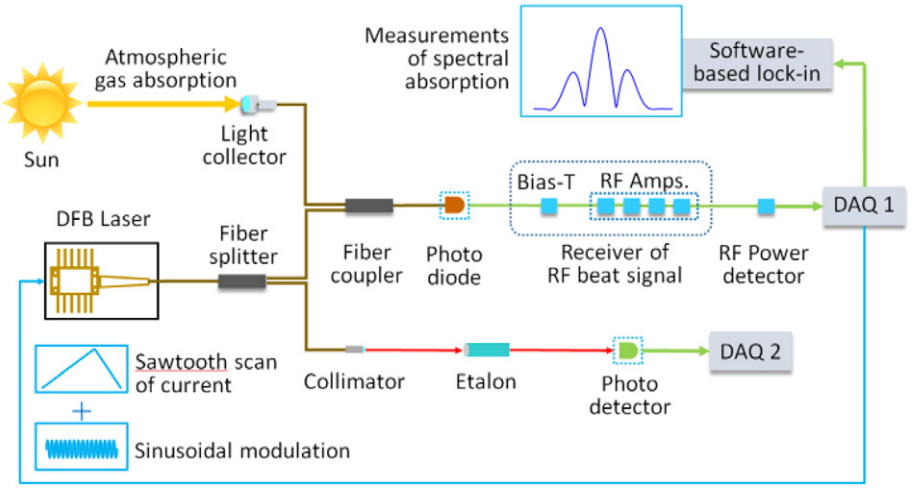

Fig. 1. Optical layout of a self-calibrated wavelength modulation laser heterodyne radiometer. DFB laser, distributed feedback laser; DAQ, data acquisition card; Bias-T, bias tee for ac coupling; RF Amps, radio frequency amplifiers.

detection process, the DC terms are generally filtered away by a high-pass or band-pass filter and the IF term is retained. The IF signal power can be detected by a Schottky diode. The voltage output signal of the Schottky diode is proportional to the IF signal power $P(t)$ or the square of the IF signal amplitude, which can be expressed as:

$$P(t) \propto \kappa^2 A_s^2 A_{LO}^2 \tag{6}$$

The above equation can be further expressed as:

$$I_H(t) \propto \beta I_S I_{LO}(t) \tag{7}$$

where $I_H(t)$ refers to the heterodyne-detected signal, β refers to a proportional constant, I_S refers to the intensity of the signal light, and $I_{LO}(t)$ refers to the intensity of the local oscillator.

If the signal light is broadband such as sun light, the total heterodyne-detected signal can be further expressed as an integration over the RF detection bandwidth:

$$I_H(t) = \beta I_{LO}(t) \int_{\nu(t)-\Delta\nu}^{\nu(t)+\Delta\nu} I_S(\nu) d\nu \tag{8}$$

where $\Delta\nu$ is the overall effective RF detection bandwidth of the system, and $\nu(t)$ is the temporal frequency of the local oscillator (laser) $I_{LO}(t)$ at time t. As the sunlight passes through the atmosphere, the captured spectral power density of the sunlight on the earth can be described by:

$$I_S(\nu) = I \exp[-\alpha(\nu)] \tag{9}$$

where I, assumed as a constant over a small wavelength range, is the spectral power density of the sunlight without absorption, and $\alpha(\nu)$ is the total absorbance along the solar radiation path. The Eq. (9) was substituted into Eq. (8):

$$I_H(t) = \beta I_{LO}(t) I \int_{\nu(t)-\Delta\nu}^{\nu(t)+\Delta\nu} exp[-\alpha(\nu)] d\nu \tag{10}$$

As the effective bandwidth $\Delta\nu$ of our combined photodiode-amplifiers for the heterodyne beat signal detection was 1 GHz, which was much narrower than spectral absorption line width, the absorption $\alpha(\nu)$ can be considered as constant within the narrow $\Delta\nu$ bandwidth. The above equation can be simplified approximately as:

$$I_H(t) = \kappa I_{LO}(t) \cdot I \cdot \ exp[-\alpha(\nu)] \cdot 2\Delta\nu = I_0(t) \ exp[-\alpha(\nu)] \tag{11}$$

where, $I_0(t)$ equals to $\kappa I_{LO}(t) \cdot I \cdot 2\Delta\nu$. Eq. (10) and Eq. (11) represent the primary signal of the heterodyne-detected spectroradiometer at the output of the RF power detector (see Fig. 1).

To achieve a self-calibrated WMS detection, the local oscillator (i.e. a DFB laser) was driven by a fast-modulated current. This lead to a simultaneous modulation of the local oscillator intensity $I_{LO}(t)$ and frequency $\nu(t)$, which resulted to:

$$I_0(t) = \overline{I_0}[1 + i_0 \cos(2\pi f t + \varphi)] \tag{12}$$

$$\nu(t) = \nu_0 + \nu_1 \cos(2\pi f t) \tag{13}$$

where $\overline{I_0}$ and ν_0 are the average value of the heterodyne-detected signal without absorption and the center frequency of the laser, respectively, f is the modulation frequency of laser drive current, i_0 is the relative modulation strength, φ refers to a phase delay, and ν_1 is the frequency modulation amplitude. Consequently, the $I_H(t)$ signal becomes modulated due to modulation of $I_{LO}(t)$ and $I_0(t)$. The R2f signal component can be obtained by using a digital lock-in amplifier to demodulate the $X_{2f}(t)$ and $Y_{2f}(t)$ components at frequency 2f by multiplying the $I_H(t)$ signal with two sets of orthogonal sine and cosine signals, respectively, and then applying a low-pass filter to remove residual high frequency components. It can be written as:

$$R2f = \sqrt{X^2{}_{2f}(t) + Y^2{}_{2f}(t)} \tag{14}$$

The R2f signal component can also be obtained by modeling it with a self-calibrated WMS technique [21]:

$$X_{2f}(t) = \frac{G\bar{I}_0}{2}\left[H_2 + \frac{i_0}{2}(H_1 + H_3)\cos\varphi\right] \tag{15}$$

$$Y_{2f}(t) = -\frac{Gi_0\bar{I}_0}{4}(H_1 - H_3)\sin\varphi \tag{16}$$

where G is the proportional coefficient, and H_k is the k^{th} order Fourier coefficient of transmittance, which can be represented as:

$$H_k = (2-\delta_{k0}) \int_{-\pi}^{\pi} \exp\{-\alpha[\nu_0 + \nu_1 \cos(2\pi f t)]\} \cos(k \cdot 2\pi f t) df t \tag{17}$$

where δ_{k0} is the Kronecker delta function.

The data processing algorithm of WMS-LHR to retrieve atmospheric CO_2 column concentration is similar to that of a self-calibrated WMS, which has been reported by us in reference [21]. A flow diagram of the data processing is illustrated in Fig. 2. The heterodyne-detected signal $I_0(t)$ and the laser frequency response $\nu(t)$ were measured/characterized separately.

In order to improve the retrieval accuracy, the details of the sunlight transmission process must be considered. In this paper, the whole atmosphere was divided into 76 layers. The vertical profiles of temperature and pressure at different altitudes were provided by the National Centers for Environment Prediction (NCEP) of USA, and the concentration of carbon dioxide was assumed to be uniform in the whole atmosphere. The simulation for the spectral absorption was calculated based on HITRAN database [22], the Line-By-Line Radiative Transfer Model (LBLRTM) [23,24], and the bandwidth $\Delta\nu$ or a measured response profile of the overall heterodyne RF power detector.

The R2f signals for the simulated and measured CO_2 spectrum were demodulated by software-based lock-in analyses. Herein, a normalization of WMS-R2f signal by the zeroth harmonic (0f) signal [18], was applied to remove the dependence of R2f signal on the laser & sunlight powers and the electronic gain. It was less suitable to use the first harmonic (1f) signal here, due to the strong absorption of CO_2 transition causing 1f signal to cross zero. The 0f signals were obtained by low-pass filtering the experimental and simulated signals. A nonlinear least-square method was used to obtain best-fit CO_2 column concentration by adjusting and matching the simulated R2f/0f signals demodulated from the simulated spectrum of CO_2 to the measured R2f/0f signals demodulated from the experimental heterodyne spectrum of CO_2.

3.2. Optimization of the modulation amplitude of WMS-LHR

Similarly as in WMS, the 2f signal amplitude of WMS-LHR strongly depends on the amplitude of the fast sinusoidal modulation of the laser drive current. In order to achieve the best performance and high SNR of the system, it is required to select the optimal modulation amplitude of the sinusoidal signal. The inset in Fig. 3 shows the experimentally measured R2f signals of atmospheric CO_2 transition at 6363.7276 cm^{-1} with different amplitude of modulation drive signals. The corresponding signal amplitudes R2f are plotted as a function of the modulation amplitude in Fig. 3. We can observe that the signal amplitude R2f grows initially as the modulation voltage increases, reaches a maximum level as the modulation amplitude equals to ~140 mV (corresponding to a laser current change of 14 mA), and then falls. All subsequent measurements of the self-calibrated wavelength modulation

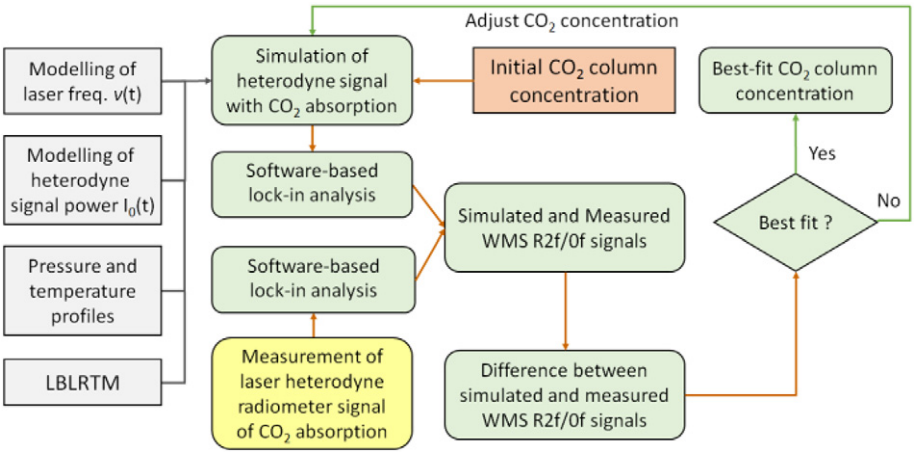

Fig. 2. Flowchart of the numerical analysis to retrieve atmospheric CO_2 column concentration.

LHR were taken at this optimal modulation amplitude. Furthermore, it should be emphasized that all the R2f signals were measured within 5 min, where the variation of solar altitude angle was less than 0.4°. Thus, the resulting changes of the solar light coupling into the optical fiber and the solar radiation path were negligible.

3.3. Simulation of heterodyne signal without absorption and scanned-modulation of laser frequency

As the laser radiation served as a local oscillator for our heterodyne-detected WMS LHR, an accurate modeling of the laser intensity and frequency responses were essential for the spectral simulation and deduction of the concentration of the target specie. Herein, the first step was to measure and model the heterodyne beat signal as the laser wavelength was fast modulated and slowly scanned. An example of raw experimental heterodyne-detected spectrum of CO_2 is shown in Fig. 4. It was measured in Hefei of China, located at 31.9°N, 117.2°E. The acquiring time was around 11:30 am on March 31, 2019, corresponding to a solar altitude angle of 61.16°. The data in Fig. 4 was obtained after averaging 1000 scans within a time of 8 s for improved SNR. The noise can be further reduced by increasing averaging time. The two strong features recorded were due to CO_2 absorption lines located at 6364.9220 cm^{-1} (R24e) and 6363.7276 cm^{-1} (R22e), respectively. Other spectral sections were absorption free. A heterodyne signal amplitude model was constructed based on the signals of these absorption-free sections by the following formula:

$$I_0(t) = A_1(t) + A_2(t) \cdot \cos(2\pi ft + \phi_1) \tag{18}$$

where $I_0(t)$ refers to the heterodyne signal amplitude; $A_1(t)$ and $A_2(t)$ refer to 4th-order polynomial and 2nd-order polynomial with adjustable coefficients, respectively; f refers to the laser modulation frequency, t refers to the scanning time, and ϕ_1 refers to a phase term. The modelled intensity profile (red line in Fig. 4), shows a good agreement with the absorption-free section of the measurements, as displayed in Fig. 4. This proves the reliability of the model function Eq. (18) for calculating absorption-free the heterodyne signal $I_0(t)$.

The temporal response of scanned-modulated laser frequency $v(t)$ was another important parameter for simulating WMS. We used a quartz etalon to accurately characterize the laser wavelength/frequency response. The free spectral range of the etalon was 0.0173 cm^{-1} (or ~520 MHz). For high precision modeling, a very sophisticated model formula was used to fit the measured etalon resonance frequencies. The scanned-modulated laser frequency can be expressed as:

$$v(t) = A_3(t) + A_4(t) \cdot \cos(2\pi ft + \varphi_1) + A_5(t) \cdot \cos(4\pi ft + \varphi_2) \tag{19}$$

where $v(t)$ refers to the laser frequency response; $A_3(t)$, $A_4(t)$ and $A_5(t)$ refers to three 3rd-order polynomials with adjustable coefficients, respectively; f refers to the modulation frequency; t refers to the scanning

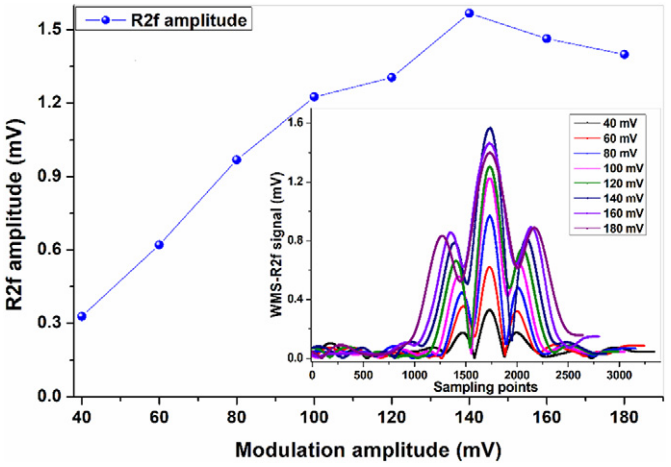

Fig. 3. The R2f amplitudes of the spectra as a function of the modulation amplitude voltage. The inset shows the corresponding experimentally measured R2f signal of atmospheric CO_2 transition at 6363.7276 cm^{-1} with different amplitudes of the sinusoidal modulation.

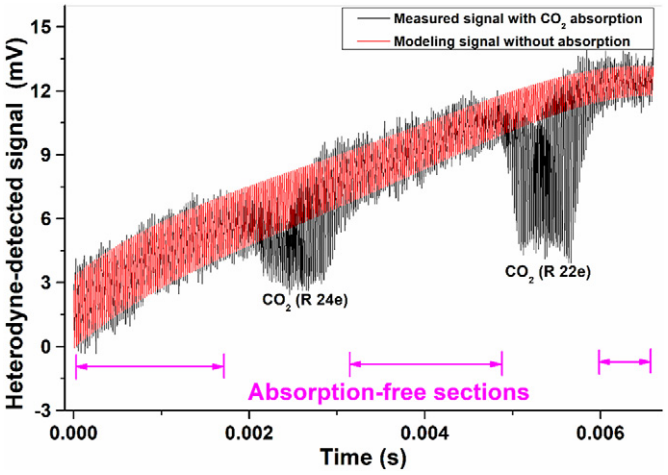

Fig. 4. Experimentally measured raw heterodyne-detected wavelength-modulation spectral signal with CO_2 absorption (black line) and the simulated absorption-free heterodyne-detected signal based on a model function (red line).

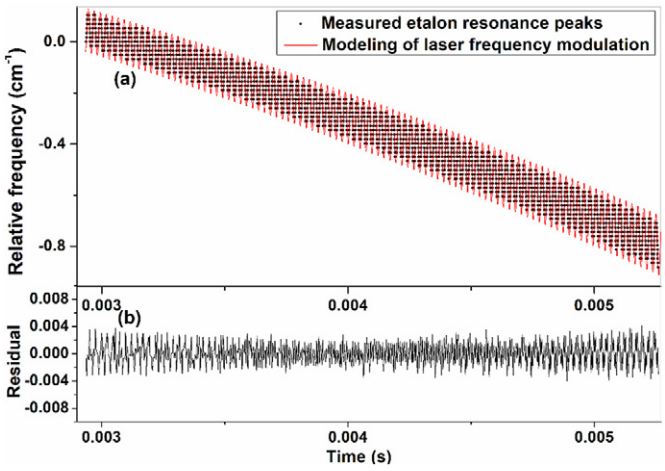

Fig. 5. (a) Experimentally measured etalon resonance peaks (gray dots) and the fitted model curve of the scanned-modulated laser frequency (red line); (b) The residual between measurements and modeling.

time; and φ_1 and φ_2 refer to phase shifts, respectively. The parameters of the model function were determined by fitting the model function to the experimentally measured etalon resonance peaks, as shown in Fig. 5(a). The residual presented in Fig. 5(b), between the values of the etalon resonance peaks and the calculated laser frequency, is within 0.004 cm^{-1}. It confirms a good accuracy of modeling function Eq. (19) for the laser frequency scan-modulation. The absolute laser frequency can be further determined during spectral fitting processes based on molecular CO_2 absorption line frequencies as reported in HITRAN database [22].

3.4. Results analysis

An example spectrum of R2f/0f signal for the CO_2 at 6363.7276 cm^{-1} is displayed in Fig. 6(a). The experimental spectrum of R2f/0f signal (in gray dots) was demodulated from the raw heterodyne-detected spectrum of CO_2 (Fig. 4) by using a software-based lock-in analyses and displayed in gray dots, whereas the best-fit curve is displayed in a red line. It shows that the fitting curve has a close consistency with the simulated WMS-R2f/0f signal. The corresponding residual is lower than 0.004, as displayed in Fig. 6(b). The column concentration of CO_2 in the atmosphere was deduced to be 413.7 ± 1.9 ppm. This value was close to monthly average CO_2 column concentration of about 412.2 ppm in Hefei, China, obtained from the satellite observation results of GOSAT [25]. The spectral signal to noise ratio (SNR) of ~333 was obtained from the ratio of the maximum of the experimental signal to the estimated fluctuation of 4E−4 for the baseline section marked with green shadow. As mentioned before, the averaging time was 8 s. In order to obtain the optimal averaging time of the system, we apply Allan deviation method to analyze the noise fluctuation of the system without the solar radiation, as depicted in Fig. 7. The performance of the laser heterodyne spectroradiometer was dominated by the noise of the laser radiation, as the solar radiation coupled to the photodiode was more than two orders of magnitude weaker. From this figure, it can be observed that the noise level of the system is 1.45E−4 with 8 s averaging time, while the noise of the system reaches the minimum level of 3.3E−5 corresponding to the averaging time of approximately 334 s. It means that the performance of the system would be improved by 4.4 times if the system operated in the optimal condition. Moreover, it is worth noting that the laser scanning frequency (125 Hz) is far higher than that of the conventional LHR [1–10]. This would offer the advantages of effectively reducing the effects of atmospheric turbulence and the drastic variation of the sunlight intensity and improving measurement time resolution. The high frequency modulation sinusoidal signal (41.22 kHz) is able to preferably suppress some 1/f electronic noises. In general, our developed WMS-LHR with software-based lock-in amplifier also shows an excellent performance comparing with the conventional LHR based on the hardware-based lock-in amplifier. This WMS-LHR has a potential to be an easily-portable, robust and high performance instrument for ground-based, airborne and spaceborne observations for the variation of the global greenhouse gases.

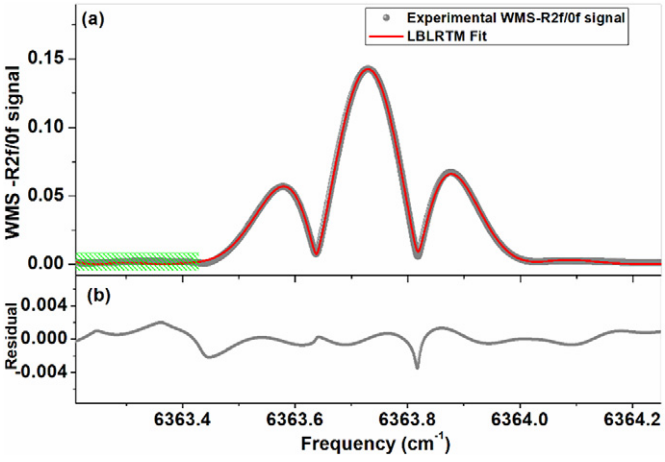

Fig. 6. (a) The demodulated WMS-R2f/0f signal (black dots) and the fitted model curve (red line); (b) The corresponding residual.

4. Conclusions

In conclusion, a self-calibrated wavelength modulation laser heterodyne radiometer using a near infrared DFB diode laser as the local oscillator, has been developed to measure atmospheric CO_2 column absorption. Unlike the conventional LHR, we also adopted software-based lock-in analysis to demodulate WMS-R2f signals and then applied normalization by 0f signal derived from filtering the measured and simulated modulation signal with a low-pass filter. The main advantage is that it can simultaneously obtain the original heterodyne signal and the demodulated harmonic signals, which are crucial for the self-calibrated wavelength modulation LHR. The process of deducing atmospheric CO_2 column concentration is analogous to normal self-calibrated WMS, where it is required to build the complex models for the absorption-free heterodyne-detected signal and for the laser frequency response to a scanned modulation, respectively. Finally, the column concentration of CO_2 was determined to be 413.7 ± 1.9 ppm by this newly developed experimental system and retrieval algorithm.

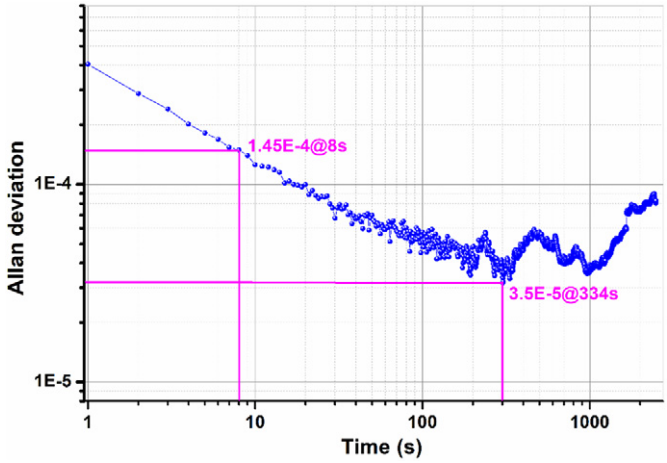

Fig. 7. Allan deviation plot of the noise level of the system without the solar radiation. It shows the dominated noise contribution by the DFB laser radiation for the heterodyne detection.

The modeling profile agrees well with the measurement WMS-R2f/0f signal. In accordance to the GOSAT observation results, the retrieved CO_2 column concentration was very close to the monthly average column concentration of CO_2 in Hefei, China. The system can also offer spectral signal with high SNR corresponding to the averaging time of 8 s. Its optimal performance can be enhanced by 4.4 times by increasing the averaging time to ~330 s. Moreover, the utilization of software-based lock-in analyses would further promote the miniaturization of a LHR, of which the system size is far smaller than that of the previously reported LHR [1–10]. This work demonstrated the feasibility of a self-calibrated wavelength modulation LHR for atmospheric investigation and the potential for ground-based, airborne and space-borne observations. As a next step, we intend to work on further improving the performance of our developed LHR. The concentration-retrieval stability will be evaluated through continuous measurements of atmospheric CO_2 column concentration using a sun tracker with high precision.

Author contributions

Hao Deng conceived and designed the system and wrote the manuscript.

Yabai He, Chenguang Yang, Ruifeng Kan supervised and managed the experimental work and manuscript.

Mingxing Li, Zhenyu Xu, Lu Yao, and Bing Chen provided the software preparation, the hardware support and the retrieval algorithm, respectively.

Declaration of competing interest

We wish to confirm that there are no known conflicts of interest associated with this publication and there has been no significant financial support for this work that could have influenced its outcome.

Acknowledgements

This work was supported by the National Key Research and Development Program of China (2016YFC1400604-02, 2016YFC0201103, 2016YFC1400604, 2016YFC0302302), and the Equipment Research and Development Program of Chinese Academy of Sciences (YJKYYQ20170062).

References

[1] E.L. Wilson, M.L. McLinden, J.H. Miller, G.R. Allan, L.E. Ott, H.R. Melroy, G.B. Clarke, Miniaturized laser heterodyne radiometer for measurements of CO_2 in the atmospheric column, Appl. Phys. B Lasers Opt. 114 (2014) 385–393.

[2] S.R. King, D.T. Hodges, T.S. Hartwick, D.H. Barker, High-resolution atmospheric-transmission measurement using a laser heterodyne radiometer, Appl. Opt. 12 (1973) 1106–1107.

[3] A. Hoffmann, N.A. Macleod, M. Huebner, D. Weidmann, Thermal infrared laser heterodyne spectroradiometry for solar occultation atmospheric CO_2 measurements, Atmos. Meas. Tech. 9 (2016) 5975.

[4] A. Hoffmann, M. Huebner, N. Macleod, D. Weidmann, Spectrally resolved thermal emission of atmospheric gases measured by laser heterodyne spectrometry, Opt. Lett. 43 (2018) 3810–3813.

[5] D. Weidmann, A. Hoffmann, N. Macleod, K. Middleton, J. Kurtz, S. Barraclough, D. Griffin, The methane isotopologues by solar occultation (miso) nanosatellite mission: spectral channel optimization and early performance analysis, Remote Sens. 9 (2017) 1073.

[6] E.L. Wilson, A.J. DiGregorio, V.J. Riot, M.S. Ammons, W.W. Bruner, D. Carter, J.P. Mao, A. Ramanathan, S.E. Strahan, L.D. Oman, C. Hoffman, R.M. Garner, A 4 U laser heterodyne radiometer for methane (CH_4) and carbon dioxide (CO_2) measurements from an occultation-viewing CubeSat, Meas. Sci. Technol. 28 (2017), 035902.

[7] D. Weidmann, W.J. Reburn, K.M. Smith, Retrieval of atmospheric ozone profiles from an infrared quantum cascade laser heterodyne radiometer: results and analysis, Appl. Opt. 46 (2007) 7162–7171.

[8] J. Wang, G. Wang, T. Tan, G. Zhu, C. Sun, Z. Cao, W. Chen, X. Gao, Mid-infrared laser heterodyne radiometer (LHR) based on a 3.53 μm room-temperature interband cascade laser, Opt. Express 27 (2019) 9610–9619.

[9] T.R. Tsai, R.A. Rose, D. Weidmann, G. Wysocki, Atmospheric vertical profiles of O_3, N_2O, CH_4, CCl_2F_2, and H_2O retrieved from external-cavity quantum-cascade laser heterodyne radiometer measurements, Appl. Opt. 51 (2012) 8779–8792.

[10] H. Deng, C. Yang, W. Wang, C. Shan, Z.Y. Xu, B. Chen, L. Yao, M. Hu, R.F. Kan, Y.B. He, Near infrared heterodyne radiometer for continuous measurements of atmospheric CO_2 column concentration, Infrared Phys. Technol. 101 (2019) 39–44.

[11] P. Martín-Mateos, O.E. Bonilla-Manrique, C. Gutiérrez-Escobero, Wavelength modulation laser heterodyne radiometry, Opt. Lett. 43 (2018) 3009–3012.

[12] P. Martín-Mateos, A. Genner, H. Moser, B. Lendl, Implementation and characterization of a thermal infrared laser heterodyne radiometer based on a wavelength modulated local oscillator laser, Opt. Express 27 (2019) 15575–15584.

[13] M. Wang, Y.J. Zhang, J.G. Liu, W.Q. Liu, R.F. Kan, T.D. Wang, D. Chen, J.Y. Chen, X.M. Wang, H. Xia, X. Fang, Applications of a tunable diode laser absorption spectrometer in monitoring greenhouse gases, Chin. Opt. Lett. 4 (2006) 363–365.

[14] R.F. Kan, W.Q. Liu, Y.J. Zhang, J.G. Liu, M. Wang, D. Chen, J.Y. Chen, Y.B. Cui, A high sensitivity spectrometer with tunable diode laser for ambient methane monitoring, Chin. Opt. Lett. 5 (2007) 54–57.

[15] L. Mei, S. Svanberg, Wavelength modulation spectroscopy - digital detection of gas absorption harmonics based on Fourier analysis, Appl. Opt. 54 (2015) 2234–2243.

[16] Y.C. Cao, N.P. Sanchez, W.Z. Jiang, R.J. Grifn, F. Xie, L.C. Hughes, C.E. Zah, F.K. Tittel, Simultaneous atmospheric nitrous oxide, methane and water vapor detection with a single continuous wave quantum cascade laser, Opt. Express 23 (2015) 2121–2132.

[17] W. Ren, W.Z. Jiang, F.K. Tittel, Single-QCL-based absorption sensor for simultaneous trace-gas detection of CH_4 and N_2O, Appl. Phys. B Lasers Opt. 117 (2014) 245–251.

[18] J. Chen, A. Hangauer, R. Strzoda, M.C. Amann, VCSEL-based calibration-free carbon monoxide sensor at 2.3 μm with in-line reference cell, Appl. Phys. B Lasers Opt. 102 (2011) 381–389.

[19] G. Zhao, W. Tan, J. Hou, X. Qiu, W. Ma, Z. Li, L. Dong, L. Zhang, W. Yin, L. Xiao, O. Axner, S. Jia, Calibration-free wavelength-modulation spectroscopy based on a swiftly determined wavelength-modulation frequency response function of a DFB laser, Opt. Express 24 (2016) 1723–1733.

[20] J.R.P. Bain, W. Johnstone, K. Ruxton, G. Stewart, M. Lengden, K. Duffin, Recovery of absolute gas absorption line shapes using tunable diode laser spectroscopy with wavelength modulation—part 2: experimental investigation, J. Lightwave Technol. 29 (2011) 987–996.

[21] M. Wei, R.F. Kan, B. Chen, Z.Y. Xu, C.G. Yang, X. Chen, H.H. Xia, M. Hu, Y. He, J.G. Liu, X.L. Xue, W. Wang, Calibration-free wavelength modulation spectroscopy for gas concentration measurements using a quantum cascade laser, Appl. Phys. B Lasers Opt. 123 (2017) 149.

[22] L.S. Rothman, I.E. Gordon, Y. Babikov, A. Barbe, D.C. Benner, P.F. Bernath, M. Birk, L. Bizzocchi, V. Boudon, L.R. Brown, A. Campargue, K. Chance, L.H. Coudert, V.M. Devi, B.J. Drouin, A. Fayt, J.M. Flaud, R.R. Gamache, J. Harrison, J.M. Hartmann, C. Hill, J.T. Hodges, D. Jacquemart, A. Jolly, J. Lamouroux, R.J. LeRoy, G. Li, D. Long, C.J. Mackie, S.T. Massie, S. Mikhailenko, H.S.P. Müller, O.V. Naumenko, A.V. Nikitin, J. Orphal, V.I. Perevalov, A. Perrin, E.R. Polovtseva, C. Richard, M.A.H. Smith, E. Starikova, K. Sung, S.A. Tashkun, J. Tennyson, G.C. Toon, V.G. Tyuterev, G. Wagner, The HITRAN2012 molecular spectroscopic database, J. Quant. Spectrosc. Radiat. Transf. 130 (2013) 4–50.

[23] S.A. Clough, M.J. Iacono, J.L. Moncet, Line-by-line calculations of atmospheric fluxes and cooling rates: application to water vapor, J. Geophys. Res. Atmos. 97 (1992) 15761–15785.

[24] S.A. Clough, M.J. Iacono, Line-by-line calculation of atmospheric fluxes and cooling rates: 2. Application to carbon dioxide, ozone, methane, nitrous oxide and the halocarbons, J. Geophys. Res. Atmos. 100 (1995) 16519–16535.

[25] GOSAT satellite observation, GOSAT data archive service, https://data2.gosat.nies.go.jp/doc/doc_tech_en.html.